

## Comparison of the Reactivity of [2.2]Paracyclophane and *p*-Xylene

Paul J. Dyson,<sup>a</sup> David G. Humphrey,<sup>b</sup> John E. McGrady,<sup>a</sup> D. Michael P. Mingos<sup>a</sup> and D. James Wilson<sup>a</sup>

<sup>a</sup> Department of Chemistry, Imperial College of Science, Technology and Medicine, South Kensington, London SW7 2AY, UK

<sup>b</sup> Christopher Ingold Laboratories, University College London, 20 Gordon Street, London WC1H 0AJ, UK

The relative abilities of [2.2]paracyclophane (C<sub>16</sub>H<sub>16</sub>) and *p*-xylene (C<sub>6</sub>H<sub>4</sub>Me<sub>2</sub>-1,4) to form arene tricarbonyl complexes from chromium hexacarbonyl has been studied in dioxane using the Strohmeier reflux method, and the rate constants contrasted. The reactions are found to proceed more quickly with [2.2]paracyclophane by *ca.* 25%. Density functional molecular-orbital calculations have rationalised this observation, and indicate that the enhanced reactivity of the [2.2]paracyclophane system relative to *p*-xylene is a consequence of repulsive interactions between the two arene decks in the former, which are relieved to some extent by co-ordination of the electron-withdrawing Cr(CO)<sub>3</sub> fragment.

[2.2]Paracyclophane was initially isolated from the high-temperature pyrolysis of *p*-xylene,<sup>1</sup> and since it was not possible, at that time, to prepare the compound by a more conventional route, it was considered that the ring strain evidently present in the molecule could only be overcome by the extreme conditions of the pyrolysis reaction. These initial inferences were proved incorrect and [2.2]paracyclophane was subsequently prepared by design *via* the intermolecular Wurtz coupling of  $\alpha,\alpha'$ -dibromo-*p*-dimethyl-benzene.<sup>2</sup>

The inter-ring distance in the [2<sub>*n*</sub>] cyclophanes is significantly smaller than the distance between the layers of graphite, and repulsions between the  $\pi$ -electron density on the two rings results in a distortion of the benzene rings from planarity towards either chair or boat conformations.<sup>3</sup> They therefore provide excellent models for the study of molecular strain and its relationship to reactivity. The conformational simplicity and unique geometry of these cyclophane molecules provide a means of investigating the transannular interactions between the aromatic rings, and yield information concerning the transmission of electronic effects from substituents on one ring to the second.

When compared to classical arenes, the most distinctive chemical property of the [2<sub>*n*</sub>]cyclophanes is the ease with which they undergo addition reactions such as Diels–Alder cycloadditions, hydrogenations and ionic additions.<sup>4</sup> However, the typical regenerative behaviour of aromatic molecules is not entirely suppressed, and substitution reactions such as bromination, Friedel–Crafts acylation and nitration are well established. Besides these reactions at the aromatic groups, reactions at the ethanediyl bridges such as cleavage, isomerisation and functionalisation also occur. The first transition-metal complex of paracyclophane, *viz.* [Cr(CO)<sub>3</sub>( $\eta$ -C<sub>16</sub>H<sub>16</sub>)], was prepared in 1960,<sup>5</sup> and in 1978 the molecular structure was established by single-crystal X-ray analysis.<sup>6</sup> Upon complexation, the two arene rings move closer together, indicating a reduction in transannular repulsions in the presence of an electron-withdrawing Cr(CO)<sub>3</sub> group. The initial work on chromium cyclophane complexes demonstrated the exciting potential of this new class of  $\pi$  ligands in organometallic chemistry, and subsequently a large number of transition metal–cyclophane complexes have been reported and recently reviewed.<sup>7</sup>

In this work we aim quantitatively to describe the different properties of [2.2]paracyclophane and *p*-xylene as ligands. The

kinetics of the reactions of the two ligands with chromium hexacarbonyl are studied, and the relative stabilities of the two products assessed. The experimentally observed differences are then interpreted with the aid of density functional molecular-orbital calculations.

### Results and Discussion

Complexes of formula [Cr(CO)<sub>3</sub>(arene)] may be prepared in high yield from the direct reaction of [Cr(CO)<sub>6</sub>] and the appropriate arene in high-boiling ethers, usually dioxane.<sup>8</sup> It is generally accepted that the substitution mechanism is first order with the rate-determining step involving dissociation of the three carbonyl ligands.<sup>9,10</sup>

We have compared the rate of reaction of two related ligands, *p*-xylene (C<sub>6</sub>H<sub>4</sub>Me<sub>2</sub>-1,4) and the highly strained ring system, [2.2]paracyclophane (C<sub>16</sub>H<sub>16</sub>), with [Cr(CO)<sub>6</sub>]. The technique involves direct reaction between [Cr(CO)<sub>6</sub>] and the appropriate arene in dioxane, using a Strohmeier reflux apparatus (see Experimental section) to prevent the loss of [Cr(CO)<sub>6</sub>] *via* sublimation. Periodic analysis of the reaction mixture at 380 K was achieved by infrared spectroscopy. The rate constants obtained for *p*-xylene and [2.2]paracyclophane were  $1.2 \times 10^{-6}$  and  $1.6 \times 10^{-6} \text{ s}^{-1}$  at 380 K, respectively.

In order to assess the relative stabilities of the two products, equimolar quantities of [Cr(CO)<sub>6</sub>], [2.2]paracyclophane and *p*-xylene were refluxed in dioxane for 5 d. The [2.2]paracyclophane derivative dominates the reaction mixture and a 10-fold excess of its product is formed. This indicates that the [2.2]paracyclophane complex is the more thermodynamically stable product.

The reaction of these arenes with [Cr(CO)<sub>6</sub>] may be greatly accelerated when carried out in a sealed system in tetrahydrofuran (thf) superheated to 125 °C by microwave dielectric heating methods (see Experimental section). A reaction time of about 40 min is sufficient for a high-yield conversion, *ca.* 90%. Clearly, this method has great potential for the preparation of a wide range of other arene chromium tricarbonyl complexes which are important reagents in the synthesis of new organic products unavailable by other routes. Many of the most desirable arenes used in this regard are poor  $\pi$  ligands and the preparation times are typically in the order of several days with conventional thermal methods.

**Density Functional Calculations.**—The bonding of a conical  $\text{Cr}(\text{CO})_3$  fragment to arene ligands has been described by a variety of authors,<sup>11</sup> and the effect of substituents on the arene ring has been examined in some depth.<sup>12</sup> No attempt has been made, however, to assess the influence on the reactivity towards a transition-metal fragment of a second arene ring lying parallel to the first, as occurs in complexes of paracyclophane. In this section we describe how calculations using density functional molecular-orbital theory have been used to consolidate the experimental observations described above, *viz.* that paracyclophane interacts more strongly than *p*-xylene with a  $\text{Cr}(\text{CO})_3$  fragment. Transannular communication between the arene rings *via* both through-space and through-bond pathways has been shown to influence the ionisation energies recorded in the photoelectron spectra of unco-ordinated cyclophanes,<sup>13</sup> and we will illustrate that the through-space mechanism is the dominant force leading to the stronger bonding of  $\text{Cr}(\text{CO})_3$  to paracyclophane relative to single arene ligands such as benzene or *p*-xylene.

The structural parameters used in the calculations are summarised in Fig. 1. In both cases, bond lengths and angles were taken from the crystal structure of  $[\text{Cr}(\text{CO})_3(\eta\text{-C}_{16}\text{H}_{16})]^{14}$  and idealised to  $C_s$  symmetry. Total energies for the association of a  $\text{Cr}(\text{CO})_3$  fragment with *p*-xylene and paracyclophane are summarised in Table 1. The calculated interaction energies clearly reproduce the experimental observations, indicating significantly stronger co-ordination of paracyclophane than *p*-xylene, the calculated association energy being  $14.5 \text{ kJ mol}^{-1}$  greater in the former. Whilst the calculated total association energies are fully in accord with experimental findings, they provide no indication of the electronic origin of the enhanced reactivity. The unusual properties of paracyclophane are clearly related to the presence of the second arene deck, but from the data summarised above it is not possible to determine the relative importance of communication between the decks *via* transannular  $\pi$ - $\pi$  repulsions (through space) and *via* the saturated ethanediyl groups (through bond). In order to determine the significance of these two mechanisms calculations have been performed on two model ligand systems in which the ethanediyl bridges of paracyclophane have been replaced by protons, thereby breaking the covalent link between the two decks [Fig. 2(b) and 2(c)]. In the distorted benzene stack [Fig. 2(b)], the benzene rings are in the same boat conformation as in paracyclophane itself. Any differences between paracyclophane and the distorted stack therefore reflect the role of the ethanediyl bridges in mediating the transannular communication. In the parallel stack [Fig. 2(a)] the distortion to the boat conformation is removed, and both rings are planar, resulting in overall  $D_{6h}$  symmetry. This second model is particularly attractive from a computational viewpoint, as, unlike the distorted stack, it retains three-fold rotational symmetry in combination with a  $\text{Cr}(\text{CO})_3$  fragment. The association energies of a  $\text{Cr}(\text{CO})_3$  fragment on the two model ligands are summarised in Table 1. The relative association energy,  $\Delta E_{\text{rel}}$ , defined as  $\Delta E_{\text{rel}} = \Delta E - \Delta E_{p\text{-xylene}}$ , is also shown in this table, providing a direct measure of the enhancement of reactivity in each case.

The value of  $\Delta E_{\text{rel}}$  for the distorted benzene stack indicates the extent of transannular communication *via* a through-space pathway only, while the corresponding value for paracyclophane represents the sum of both through-space and through-bond pathways. The larger value of  $\Delta E_{\text{rel}}$  for the distorted stack (relative to paracyclophane) indicates that the saturated ethanediyl bridges actually attenuate the influence of one arene deck on the other, rather than enhancing it. Thus, it appears that a type of synergic effect is in operation, whereby the enhanced reactivity arising as a consequence of the through-space pathway is reduced somewhat by the ethanediyl bridges. Finally, it is noteworthy that  $\Delta E_{\text{rel}}$  is very similar for both distorted and parallel stack ligands, indicating that the distortion from planarity to a boat conformation has a

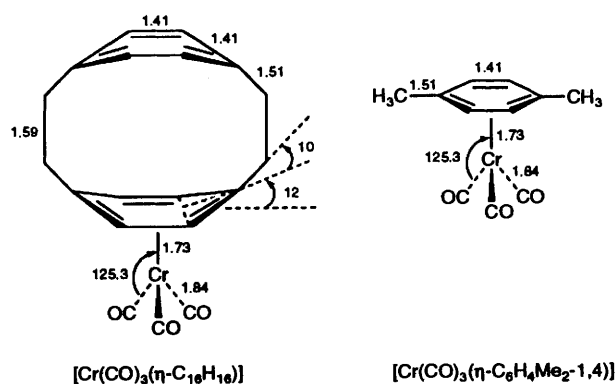


Fig. 1 Structural parameters (distances in Å, angles in °) used in calculations on paracyclophane and *p*-xylene complexes of  $\text{Cr}(\text{CO})_3$

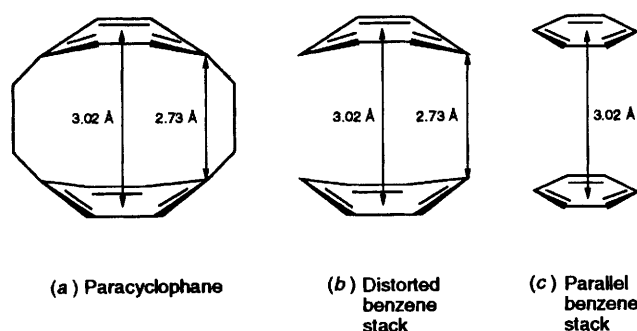


Fig. 2 Idealised ligands used to model the properties of paracyclophane

Table 1 Association energies of a  $\text{Cr}(\text{CO})_3$  fragment with *p*-xylene, paracyclophane and the model ligands shown in Fig. 2

Complex	$\Delta E / \text{kJ mol}^{-1}$	$\Delta E_{\text{rel}} / \text{kJ mol}^{-1}$
$\text{Cr}(\text{CO})_3(\eta\text{-C}_6\text{H}_4\text{Me}_2\text{-1,4})$	-241.3	0.0
$\text{Cr}(\text{CO})_3(\eta\text{-C}_{16}\text{H}_{16})$	-255.8	-14.5
$\text{Cr}(\text{CO})_3(\text{C}_6\text{H}_6)_2$ - distorted stack	-263.6	-22.3
$\text{Cr}(\text{CO})_3(\text{C}_6\text{H}_6)_2$ - parallel stack	-265.4	-24.1

negligible effect on the properties of the ligand. Consequently the parallel stack system, with its attendant computational benefits, was used in all subsequent calculations.

Having established that the through-space interaction is responsible for the enhanced reactivity of paracyclophane we are now in a position to relate this phenomenon to the transannular  $\pi$ - $\pi$  repulsions between the benzene rings. Fig. 3 summarises a hypothetical scheme for the formation of  $[\text{Cr}(\text{CO})_3(\text{C}_6\text{H}_{12})]$  from a  $\text{Cr}(\text{CO})_3$  fragment and two isolated benzene rings where  $\text{C}_6\text{H}_{12}$  represents a pair of benzene rings stacked upon each other at the appropriate inter-ring distance. The steps labelled  $\Delta E_{\text{ass}}^1$  and  $\Delta E_{\text{ass}}^2$  represent the association energies of  $\text{Cr}(\text{CO})_3$  with benzene and dibenzene, respectively. Those labelled  $\Delta E_{\pi-\pi}^1$  and  $\Delta E_{\pi-\pi}^2$  represent the repulsive interaction between two benzene rings, with a  $\text{Cr}(\text{CO})_3$  fragment coordinated to one ring in the latter case. From Fig. 3 it is apparent that the enhanced reactivity of dibenzene over benzene ( $\Delta E_{\text{ass}}^1 - \Delta E_{\text{ass}}^2$ ) is directly related to changes in the transannular  $\pi$ - $\pi$  interactions ( $\Delta E_{\pi-\pi}^1 - \Delta E_{\pi-\pi}^2$ ) *via* equation (1).

$$\Delta E_{\pi-\pi}^1 - \Delta E_{\pi-\pi}^2 = \Delta E_{\text{ass}}^1 - \Delta E_{\text{ass}}^2 \quad (1)$$

The components of the association energies and  $\pi$ - $\pi$  interaction energies, calculated using the transition-state

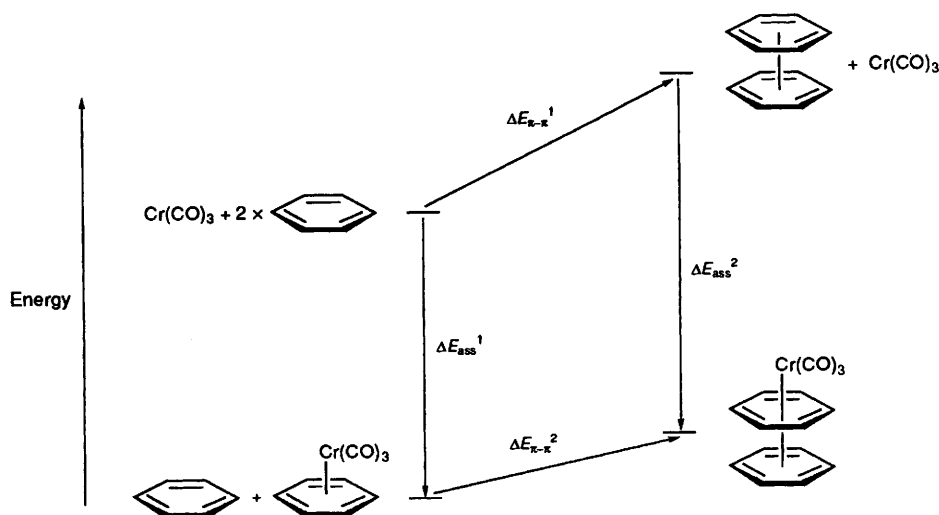


Fig. 3 Thermodynamic cycle relating metal-ligand association energies to transannular  $\pi$ - $\pi$  repulsions

Table 2 Components of the total energies  $\Delta E_{\text{ass}}^{1,2}$  and  $\Delta E_{\pi-\pi}^{1,2}$  defined in Fig. 3

	$\Delta E_{\text{el}}$	$\Delta E_{\text{xrp}}$	$\Delta E_{\text{oi}}$	$\Delta E_{\text{tot}}$
$\Delta E_{\text{ass}}^1$	-474.5	737.6	-512.1	-239.4
$\Delta E_{\text{ass}}^2$	-504.6	751.9	-512.7	-265.4
$\Delta E_{\pi-\pi}^1$	-107.5	186.9	-25.6	53.8
$\Delta E_{\pi-\pi}^2$	-102.9	164.7	-34.6	27.3

approximation of Ziegler and Rauk,<sup>14</sup> are summarised in Table 2. The reduction in  $\pi$ - $\pi$  repulsion energy,  $\Delta E_{\pi-\pi}^1 - \Delta E_{\pi-\pi}^2$ , is dominated by changes in the exchange repulsion term, which is related to the destabilising overlap of the  $\pi$  electrons on the two benzene rings. To understand the connection between this  $\pi$ - $\pi$  exchange repulsion and the enhanced reactivity of paracyclophane we must consider the deformation-density maps for the steps associated with  $\Delta E_{\pi-\pi}^1$  and  $\Delta E_{\pi-\pi}^2$ , illustrated in Fig. 4. The  $\pi$ - $\pi$  repulsions between two uncoordinated benzene rings result in a displacement of electron density from the transannular region to the outer faces of the benzene rings; this effect is clearly shown in the deformation-density map in Fig. 4(a). The build-up of negative charge on the outer faces of the arene rings increases the nucleophilicity of the dibenzene system, and consequently the reaction with an electrophilic species such as  $[\text{Cr}(\text{CO})_6]$  is accelerated.

The greater thermodynamic stability of the paracyclophane complex is due to the reduction in  $\pi$ - $\pi$  repulsions in the coordinated species, a direct consequence of the electron-withdrawing nature of the  $\text{Cr}(\text{CO})_3$  group. This effect is illustrated by a comparison of Fig. 4(a) and 4(b), which indicates that substantially less electron density is forced out of the transannular region when one of the benzene rings is coordinated to a metal fragment. The preference of the metal fragment to bind to paracyclophane is clearly dependent on the ability of the metal to withdraw electron density from the aromatic system, and we would therefore anticipate that the enhanced reactivity of paracyclophane would be less pronounced as the metal fragment becomes less electron deficient.

## Conclusion

The presence of two arene rings lying parallel to each other at a distance considerably less than a typical van der Waals contact confers unusual properties upon [2.2]paracyclophane, which is

found to be markedly more reactive towards  $[\text{Cr}(\text{CO})_6]$  than the related single-deck arene, *p*-xylene. [2.2]Paracyclophane reacts more quickly than *p*-xylene; kinetic measurements have established that the rate constant is larger by some 25% at 380 K. When equimolar amounts of both arenes are made available in the same reaction mixture the [2.2]paracyclophane complex is found to dominate the equilibrium mixture and the ratio of the [2.2]paracyclophane to *p*-xylene products is 10:1. The increased rate of reaction of [2.2]paracyclophane with  $[\text{Cr}(\text{CO})_6]$  stems from the  $\pi$ - $\pi$  repulsions between the arene rings, which increase the electron density on the outer faces of the ligand, thereby increasing its nucleophilicity relative to benzene. The increased thermodynamic stability of the paracyclophane complex arises from the reduction in these  $\pi$ - $\pi$  repulsions in the complex, a consequence of the electron-withdrawing nature of the metal fragment.

## Experimental

**Reactivity Studies.**—The Strohmeier reflux method was used in all reactions in order to ensure that the  $[\text{Cr}(\text{CO})_6]$  was not lost from the reaction mixture by sublimation.<sup>15</sup> The apparatus consisted of two reflux condensers connected in series, the lower one without cooling water, the upper one with cooling water. Any  $[\text{Cr}(\text{CO})_6]$  which sublimes onto the lower condenser is then washed back into the reaction vessel by the solvent which condenses on the upper condenser. This method has been described in detail elsewhere. Materials were used as supplied except for 1,4-dioxane which was distilled over sodium. Solution infrared spectra ( $1.0 \text{ cm}^{-1}$  resolution) were recorded in a Specac solution cell (KBr windows) of path length 0.1 mm against a neat solvent background, using a dry-air purged Nicolet 750 FT spectrometer.

In a typical kinetics run,  $[\text{Cr}(\text{CO})_6]$  (80 mg, 0.36 mmol) and the appropriate arene (0.36 mmol) were combined in a Schlenk flask and the flask purged. Deoxygenated 1,4-dioxane ( $50 \text{ cm}^3$ ) was added to this mixture and the solution heated to reflux (solvent temperature  $\approx 380 \text{ K}$ ). Aliquots ( $0.1 \text{ cm}^3$ ) were periodically withdrawn from the reaction mixture over the following 25 h, and the infrared spectrum of each recorded immediately after sampling. The rate of reaction of  $[\text{Cr}(\text{CO})_6]$  with the arenes was determined by monitoring the disappearance of  $\nu(\text{CO})$  from  $[\text{Cr}(\text{CO})_6]$  at  $1980 \text{ cm}^{-1}$  ( $t_{1u}$ ) with time. The concentration of  $[\text{Cr}(\text{CO})_6]$  was proportional to the absorbance at the analytical wavenumber, given that Beers law holds over the concentration range used. Plots of  $\ln(A_t/A_0)$  versus time (where  $A_t$  = absorbance at time  $t$  and  $A_0$  = initial

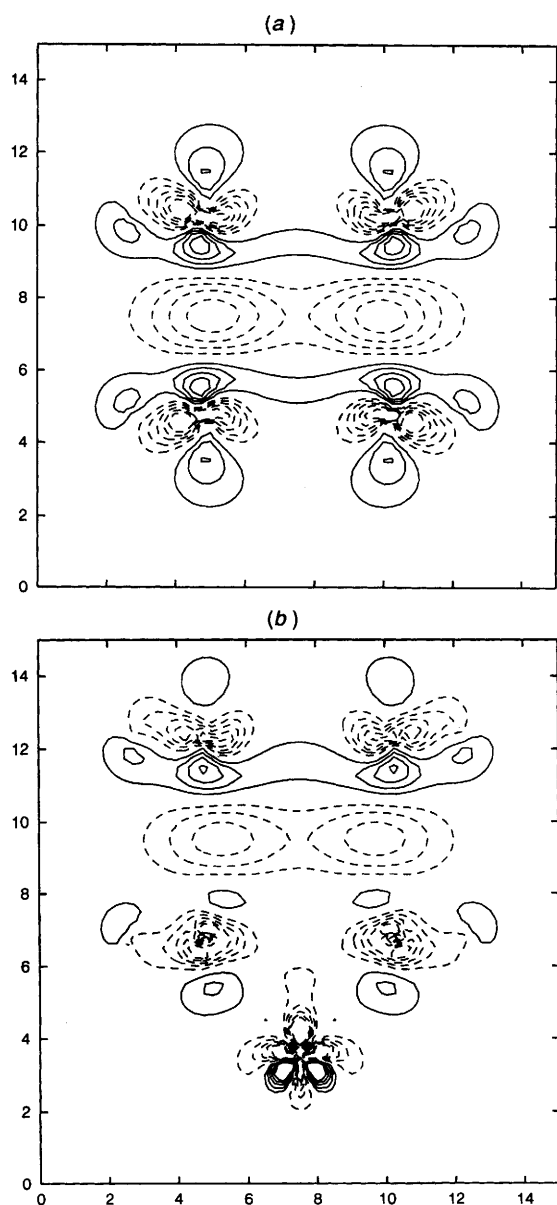


Fig. 4 Deformation-density plots for the formation of (a)  $(C_6H_6)_2$  from  $2 \times C_6H_6$  and (b)  $[Cr(CO)_3\{(C_6H_6)_2\}]$  from  $[Cr(CO)_3(C_6H_6)] + C_6H_6$ , shown in a plane containing the carbon atoms at the 1,4 positions of each ring. Distances are in atomic units; successive contours correspond to  $\pm 0.0005$ ,  $\pm 0.0010$ ,  $\pm 0.0015$ ,  $\pm 0.0020$  and  $\pm 0.0025$  electron  $au^{-3}$  (1 au = 0.529 Å)

absorbance) gave first-order rate constants as listed in the text. Reagent concentrations were not corrected to account for the loss of material contained in each aliquot sampled.

**Microwave Synthesis.**—Reactions were carried out using a CEM MDS-2000 microwave oven with the power level selected at 650(50) W. The reactants were placed in a poly(tetrafluoroethylene) liner and sealed inside a Teflon reaction vessel (CEM-lined digestion vessel, 200 cm<sup>3</sup> capacity). The reaction vessel could then be transported to the microwave oven where it was connected to a temperature probe. The outlet to which the pressure monitor is attached was closed, and the reaction was controlled *via* the temperature probe by means of a built-in computer. The equipment has been described previously.<sup>16</sup> In a typical reaction  $[Cr(CO)_6]$  (100 mg), [2.2]paracyclophane (100 mg, 1 mol equivalent) and thf (25 cm<sup>3</sup>) were placed in the reaction vessel and heated to 140 °C for 40 min. After

cooling to room temperature, the yellow solution was transferred to a flask and the solvent removed under vacuum. The yellow solid was characterised by infrared spectroscopy as  $[Cr(CO)_6(C_{16}H_{16})]$  (280 mg, 91%).

**Computational Details.**—**Molecular-orbital calculations.** All calculations were based on approximate density functional theory using the Amsterdam density functional (ADF) package developed by Baerends and co-workers.<sup>17</sup> The local-density approximation was employed using the parametrisation of Vosko, *et al.*<sup>18</sup> for the exchange-correlation potential. Gradient corrections to exchange (Becke<sup>19</sup>) and correlation (Perdew<sup>20</sup>) functionals were included at each iteration of the self-consistent field (SCF) procedure. The valence orbitals of Cr (3d, 4s, 4p) were represented by a triple- $\zeta$  Slater-type orbital (STO) basis set. A double- $\zeta$  basis was employed for the 2s and 2p orbitals of C and O and the 1s orbital of H. For C and O this basis was augmented by a single 3d function, while for hydrogen a 2p orbital was used for polarisation. All electrons in lower shells were considered as core and treated according to the frozen-core approximation of Baerends *et al.*<sup>21</sup> An auxiliary set of s, p, d, f and g STO functions, centred on all nuclei, was used to fit the molecular density.

**Energy-decomposition scheme.** The total bonding energies presented were evaluated using an energy-decomposition scheme based on the generalised transition-state method developed by Ziegler and Rauk.<sup>14</sup> This method decomposes the total energy into steric and electronic components. The transition-state method considers the molecule to be composed of atomic or molecular fragments, and the interaction between the fragments is given by eqn. (2). The Pauli exchange

$$\Delta E_{\text{int}} = \Delta E_{\text{el}} + \Delta E_{\text{xrp}} + \Delta E_{\text{oi}} \quad (2)$$

interaction,  $\Delta E_{\text{xrp}}$ , is directly related to the four-electron two-orbital destabilising interactions, while  $\Delta E_{\text{el}}$  is the electrostatic interaction between the fragments. The orbital-interaction term,  $\Delta E_{\text{oi}}$ , arises through the interaction between the occupied and virtual orbitals on the two fragments.

#### Acknowledgements

D. G. H. thanks the Ramsay Memorial Fellowship Trust for a British Ramsay Fellowship. The British Biological Science Research Council are thanked for financial assistance, and BP plc for endowment of a chair (to D. M. P. M.).

#### References

- 1 C. J. Brown and A. C. Farthing, *Nature (London)*, 1949, **164**, 915.
- 2 D. J. Cram and H. Steinberg, *J. Am. Chem. Soc.*, 1951, **73**, 5691.
- 3 D. J. Cram and J. M. Cram, *Acc. Chem. Res.*, 1971, **4**, 204 and refs. therein.
- 4 J. Kleinschroth and H. Hopf, *Angew. Chem., Int. Ed. Engl.*, 1982, **21**, 469 and refs. therein.
- 5 D. J. Cram and D. I. Wilkinson, *J. Am. Chem. Soc.*, 1960, **82**, 5721.
- 6 Y. Kai, N. Yasuoka and N. Kasai, *Acta Crystallogr., Sect. B*, 1978, **34**, 2840.
- 7 J. Schulz and F. Vögtle, *Top. Curr. Chem.*, 1994, **172**, 41.
- 8 M. Vemura, *Adv. Metal-Org. Chem.*, 1991, **2**, 195.
- 9 E. O. Fischer, K. Ofele, H. Essler, W. Frohlich, J. P. Mortensen and W. Semmlinger, *Chem. Ber.*, 1958, **91**, 2763.
- 10 D. A. Brown, N. J. Gogan and H. Sloan, *J. Chem. Soc.*, 1965, 6873.
- 11 B. P. Byers and M. B. Hall, *Organometallics*, 1987, **6**, 2319; R. Hoffman and T. A. Albright, *J. Am. Chem. Soc.*, 1977, **99**, 7546.
- 12 A. D. Hunter, V. Mozol and S. D. Tsai, *Organometallics*, 1992, **11**, 1150; A. D. Hunter, L. Shilliday, W. S. Furey and M. J. Zaworotko, *Organometallics*, 1992, **11**, 2251; D. Rooney, J. Chaiken and D. Driscoll, *Inorg. Chem.*, 1987, **26**, 3939.
- 13 R. Gleiter, W. Schäfer, G. Krennrich and H. Sakurai, *J. Am. Chem. Soc.*, 1988, **110**, 4117; E. Heilbronner and Z. Yang, *Top. Curr. Chem.*, 1973, **115**, 1.

- 14 T. Ziegler and A. Rauk, *Theor. Chim. Acta*, 1977, **46**, 1.
- 15 W. Strohmeier, *Chem. Ber.*, 1961, **94**, 2490.
- 16 D. M. P. Mingos and D. R. Baghurst, *Chem. Soc. Rev.*, 1991, **20**, 1.
- 17 P. M. Boerrigter, G. te Velde and E. J. Baerends, *Int. J. Quantum Chem. Symp.*, 1988, **33**, 307.
- 18 S. H. Vosko, L. Wilk and M. Nusair, *Can. J. Phys.*, 1980, **58**, 1200.
- 19 A. D. Becke, *Phys. Rev. A*, 1988, **38**, 3098.
- 20 J. P. Perdew, *Phys. Rev. B*, 1986, **33**, 8822.
- 21 E. J. Baerends, D. E. Ellis and P. Ros, *Chem. Phys.*, 1973, **2**, 41.

Received 4th July 1995; Paper 5/04336K